Int. J. Environ. Sci. Technol. (2015) 12:2777–2790
DOI 10.1007/s13762-014-0680-2

ORIGINAL PAPER

Determination of aerosol deliquescence and crystallization relative humidity for energy saving in free-cooled data centers

L. Ferrero · L. D'Angelo · G. Rovelli · G. Sangiorgi · M. G. Perrone · M. Moscatelli · M. Casati · V. Rozzoni · E. Bolzacchini

Received: 22 November 2013 / Revised: 7 May 2014 / Accepted: 23 September 2014 / Published online: 1 October 2014

Abstract This study examines an innovative application of the aerosol deliquescence and crystallization determination, for corrosion prevention and energy-saving strategies in free-cooled data centers. Aerosol deliquescence and crystallization were investigated by combining standardized aerosol sampling techniques (i.e. EN-14907) with the assessment of the electrical effects of aerosol, while varying relative humidity within a specially designed aerosol exposure chamber. Aerosol samples collected in the Po Valley (Northern Italy) were analysed; a clearly defined hysteresis cycle (deliquescence and crystallization at 60.5 ± 0.8 and 47.9 ± 0.7 % of RH, respectively) was found. Results were applied to a data center designed for the Italian National Oil and Gas Company, making it possible to identify a critical area for direct free cooling at this data center. As a result, aerosol hydration was avoided (thus preventing aerosol from damaging electrical components) and a large amount of energy saved (using free cooling instead of air-conditioning); the potential energy saving achieved in this way was 79 % (compared to the energy consumption of a traditional air-conditioning system): 215 GWh of energy was saved, and 78 fewer kt of equivalent CO_2 was emitted per year. Moreover, in order to evaluate whether a real-time estimation of the aerosol hydration state within a data center could be performed, measured deliquescence and crystallization were compared through simulations performed using three different models: two thermodynamic models for deliquescence and a parametric model for crystallization. The results obtained tend to converge in terms of deliquescence, whereas in the case of crystallization, they failed to effectively simulate experimental aerosol behaviour.

Keywords Conductivity · Aerosol chamber · Hygroscopicity · Models · Energy · Carbon footprint

Introduction

The level of aerosol hydration impacts a wide range of aerosol properties (both physical–chemical and optical) and processes (multiphase reactions, corrosion, etc.) and is of fundamental importance in several areas of aerosol research (such as climate forcing, visibility, atmospheric aerosol chemistry, energy saving in data centers, nuclear waste management, etc.) (Ferrero et al. 2011a, 2013; Di Nicolantonio et al. 2009; Randriamiarisoa et al. 2006; Syed 2006; Martin 2000; Martin et al. 2003; Rood et al. 1987).

The aerosol hydration level depends on the relative humidity (RH) to which an aerosol particle is exposed in the atmosphere compared to the values of the aerosol's deliquescence relative humidity (DRH) and crystallization relative humidity (CRH) in function of the RH history at atmospheric temperature (*T*). In particular, during a humidification process (i.e. an increase in RH), the aerosol is solid until RH reaches DRH: the aerosol then starts to absorbs water, producing a saturated aqueous solution; a further increase in the ambient RH leads to hygroscopic growth due to the continuous condensation of water. The

---

Electronic supplementary material The online version of this article (doi:10.1007/s13762-014-0680-2) contains supplementary material, which is available to authorized users.

L. Ferrero (✉) · L. D'Angelo · G. Rovelli · G. Sangiorgi · M. G. Perrone · M. Moscatelli · M. Casati · V. Rozzoni · E. Bolzacchini
Department of Earth and Environmental Sciences, POLARIS Research Centre, University of Milano-Bicocca, P.zza della Scienza 1, 20126 Milan, Italy
e-mail: luca.ferrero@unimib.it

reverse happens during dehumidification (i.e. a reduction in RH starting from a value above DRH): evaporation takes place and the aerosol particle remains supersaturated until the CRH (lower than the DRH) is reached and crystallization occurs, leading once again to a dry state through a cycle of hysteresis (Randriamiarisoa et al. 2006; Martin 2000; Martin et al. 2003; Seinfeld and Pandis 1998).

The aerosol's ability to promote "failures" in electronic equipment as a result of its hydration level is widely reported in the literature (Shehabi 2009; Shields and Weschler 1998); thus, aerosol hysteresis becomes crucial for data centers (DCs) characterized by the high density of information technology (IT: data storage, computational power, global networks, etc.) (Shehabi et al. 2008). If aerosol deposits on electronic circuitry and the ambient RH exceeds the aerosol DRH, or remains higher than the aerosol CRH (while decreasing from above the DRH), the water-soluble ionic compounds are dissociated and the aerosol is then electrically conductive and corrosive (Song et al. 2013; Shehabi et al. 2008; Tencer 2008; Syed 2006; Yang et al. 2006; Lobnig et al. 1994). This behaviour constitutes a serious risk in DCs because, as Leiva et al. (2013) have shown, atmospheric pollution is often related with high concentrations of water-soluble inorganic ions.

Thus, the American Society of Heating, Refrigerating and Air-Conditioning Engineers (ASHRAE) Technical Committee 9.9 has published guidelines on the aerosol contamination and thermodynamic conditions permitted in DCs (ASHRAE 2011 and 2009). In order to comply with the aforementioned guidelines, traditional DCs cool the hot air produced by IT, mainly by using air-conditioning units (through a closed-loop air cycle) which also enable the RH of the air to be controlled; however, a considerable amount of energy (~35–50 %) is lost in the cooling process (Greenberg et al. 2006; Tschudi et al. 2004). As a result, considering both the energy lost and the energy needed to operate the IT equipment, DCs are responsible for approximately 2 % of worldwide electricity consumption (27 % of this in Western Europe) (Koomey 2008); a further fivefold increase is expected by the year 2025 (Otagiri and Kutami 2010).

Thus, solutions capable of offsetting the financial and environmental costs of DCs are required. As reported by Hong et al. (2012), a reduction in electricity consumption represents an equivalent reduction in greenhouse gas emissions. The need for both energy saving and greenhouse gas reduction is also an integral part of new European regulations (i.e. EU/27/2012) designed to encourage the development and introduction of innovative technologies.

In order to reach this goal, the IT in DCs could be cooled directly using outside air in favourable weather conditions [direct free cooling (DFC)]. However, while this be an attractive solution, DFC runs the risk of introducing aerosol particles (Shehabi et al. 2008): this risk is instead avoided in the traditional air-conditioning cooling of DCs, which is, however, responsible for their substantial energy consumption.

As has been recently demonstrated, this deadlock can be overcome with the help of on-site knowledge of the aerosol's properties, so as to avoid aerosol hydration and corrosion (Ferrero et al. 2013).

As a matter of fact, ASHRAE guidelines (regarding humidity) are quite general and only indicate the need for DRH estimations by means of conductivity measurements carried out on dust "brushed off" a server's surface, but fail to take account of any CRH estimation.

In recent years, conductivity measurements have been employed by Yang et al. (2006) and, more recently, by Song et al. (2013), in order to determine DRH. Yang et al. (2006) only investigated the behaviour of pure salt solutions adsorbed on a filter paper; no ambient aerosol samples were examined. Conversely, Song et al. (2013) performed conductivity measurements on two ambient aerosol samples, the collection of which, however, according to ASHRAE (2011) guidelines, is devoid of any standardization. Neither of these studies took any account of CRH estimation.

However, as stated above, only a knowledge of both DRH and CRH determine whether the aerosol is dry or hydrated at a given ambient relative humidity (RH) and temperature (*T*) (Randriamiarisoa et al. 2006; Martin 2000; Martin et al. 2003; Seinfeld and Pandis 1998; Potukuchi and Wexler 1995); thus, the CRH is not only a crucial parameter, but also a fundamental concept that has to be has to be taken into account in order to prevent DC corrosion.

Finally, no study has yet addressed the possibility of estimating DRH and CRH within a DC in real time, via modelling activity, starting from a knowledge of the aerosol's chemistry, the determination of which at a high time resolution is not currently a limiting factor (Jayne et al. 2000).

Hence, this paper fills the aforementioned gaps by: (1) measuring the aerosol's DRHs and CRHs by means of conductivity leaks on the main, widely used aerosol sampling supports (in compliance with EN-14907), thus permitting the development of routine, cost-effective monitoring for both DRH and CRH; (2) comparing the experimental results with modelled outcomes, using E-AIM II (Pathak et al. 2004; Clegg et al. 1998), ISORROPIA II (Fountoukis and Nenes 2007) and a parametric model (Martin et al. 2003) in order to lay the foundation for the real-time estimation of the aerosol hydration state within a DC, from a knowledge of the aerosol's chemistry; (3) applying the obtained results (DRHs and CRHs from the Po Valley) to the design of a

DC created for the Italian National Hydrocarbon Institution (Eni) (5,200 m^2 of servers installed, which came into operation in December 2013).

In this application, an accurate determination of both DRH and CRH made it possible to optimize the DFC operating cycle in order to prevent aerosol hydration (and thus corrosion), while at the same time achieving high levels of energy saving.

To investigate the aforementioned issues, this study reports results from a research project conducted in the Milan area (situated in the centre of the Po Valley), on particulate matter (PM) samples collected between 2006 and 2013 and analysed in an aerosol exposure chamber (AEC) specifically designed for this purpose.

Materials and methods

This section describes the measurement of aerosol DRH and CRH using an AEC, the determination of the aerosol's chemistry, and the use thereof as an input for DRH and CRH modelling. Moreover, a description is provided of the DC case study and the ASHRAE (2011) guidelines.

DRH and CRH measurements

Aerosol sampling

As mentioned in the introduction, the ASHRAE (2011) recommends that aerosol for DRH estimation be collected by brushing it off a surface; however, this method of collection lacks any degree of standardization and can affect the result obtained. One way of overcoming this problem is to sample the aerosol using those standard methods adopted for atmospheric PM determination both in Europe and in the USA, that is, the benchmark gravimetric method involving the collection of PM on a filter support. Moreover, aerosol samples should also be collected in order to determine both DRH and CRH for any aerosol size capable of getting into DCs during DFC operations. In this respect, as ASHRAE (2009 and 2011) and other authors have mentioned (Ferrero et al. 2013; Shehabi 2009; Shehabi et al. 2008, 2010), a filtering system consisting of MERV13 filters (MERV = Minimum Efficiency Reported Value) is recommended for DCs. The MERV13 filter's efficiency is a function of particle size and aerosol mass loading: efficiency increases with increasing particle size, up to 100 % at 3 μm (Nazaroff 2004). Hence, DRH and CRH need to be measured for fine aerosol particles (<3 μm), which are capable of getting into a DC despite the filters.

For this reason, we firstly suggest the standardization of aerosol sampling in relation to the $PM_{2.5}$ aerosol ensemble, as collection efficiency decreases with increasing particle size (50 % at 2.5 μm) and drops to zero above 3 μm. This approach makes it possible to collect particles smaller than those guaranteeing the 100 % efficiency of the MERV13 filters usually installed in a DC. Moreover, $PM_{2.5}$ is internationally defined and standardized (EN-14907 for Europe and EPA CFR 40 for the USA).

Thus, for the purposes of this work, $PM_{2.5}$ samples, gravimetrically collected during the period 2006–2009 (in compliance with EN-14907), were used. The $PM_{2.5}$ was sampled using the FAI-Hydra dual channel low-volume-sampler (LVS; 2.3 m^3 h^{-1}, 24 h of sampling time, 47 mm PTFE filters with an available sampling diameter of 39 mm). The $PM_{2.5}$ samples were collected in Milan, at the Torre Sarca site (TS; 45°31′19″N, 9°12′46″E) situated in the centre of the Po Valley, a European aerosol pollution hotspot (Ferrero et al. 2007, 2012; Carbone et al. 2010; Rodriguez et al. 2007).

TS has been active since 2005 on the Milano-Bicocca University campus. A full description of the site and the related aerosol properties (chemistry, sources, vertical profiles and toxicity) is given in Ferrero et al. (2010, 2011b, 2014), in Perrone et al. (2012, 2013), and in Sangiorgi et al. (2011).

After collecting the $PM_{2.5}$ samples, the filters were dried out and stored in darkness at −20 °C at the University of Milano-Bicocca's Filter Bank. This Filter Bank has been specially designed for the collection and storage of PM samples to be used later (after sampling) in order to investigate new aspects of aerosol science.

In order to both measure and model the aerosol's DRH and CRH, the $PM_{2.5}$ filters that had been collected were cut into two halves; the first half was analysed in an AEC, while the second half was utilized to determine the aerosol's chemistry.

The uniformity of PM samples on filters has been examined in a previous work (Owoade et al. 2006).

Aerosol exposure chamber and conductivity measurements

The AEC was specifically designed for the purpose of this experiment, in order to perform electrical conductivity measurements on aerosol samples while varying RH. The AEC is a 1 m^3, hermetically sealed chamber equipped with inert PTFE bypasses enabling measuring and phasing operations to be performed in the presence of moist or dry air. Up to six aerosol samples positioned on special PTFE supports, and provided with a pair of electrodes each, may be housed inside the AEC. A diagram of the AEC is given in Figure S1 of the supplementary material.

For the purpose of the present application, RH was varied within the AEC by 1 % at a time, during both humidification and dehumidification. This resulted in more accurate levels of DRH and CRH estimation than that of the lower resolution (~3–5 %) reported in Yang et al. (2006) and Song et al. (2013). The humidification ramp was achieved by increasing the RH in the AEC by means of an evaporating system for ultra-pure water (Milli-Q®; 18.2 MΩ cm @ 25 °C; Water Purification System, Millipore, Bedford, MA, USA); conversely, dehumidification was performed by phasing in pure air (Aria Zero®, SapioS.r.l.) until complete dryness had been achieved. As a result, the water uptake on aerosol samples during deliquescence promotes the solubilization of water-soluble ionic compounds, resulting in a sharp change in aerosol conductivity. The opposite happens during crystallization.

During both DRH and CRH measurements, temperature (*T*) was maintained constant at 25 °C. 25 °C was chosen as this is the temperature of the supply of cooling air within the DC reported in this work as a case study (see the "DC's case study" section); the importance of maintaining *T* constant during the measuring process derives from the observation made in the literature that both DRH and CRH are functions of *T* (Onasch et al. 1999; Seinfeld and Pandis 1998).

Thus, RH and *T* were constantly monitored (at a resolution of 0.25 % for RH and of 0.035 °C for *T*) while performing the experiments, using a thermo-hygrometric sensor (DMA672, LSI-Lastem) inserted into one of the PTFE bypasses. This sensor was linked to an M-Log (ELO008 Data-Logger, LSI-Lastem), which recorded RH and *T* with a time resolution of 1 s.

DRH and CRH were determined in the AEC by means of electrical conductivity (*G*) measurements performed during humidification and dehumidification, by means of an HP 3421A Module. For every 1 % step in RH in the AEC, three conductivity measurements were taken for each aerosol sample and then these measurements were averaged. The measured electrical conductivity curves enabled DRH and CRH to be determined; the methodology, together with the calculation of the minimum aerosol loading required to successfully perform conductivity measurements, is discussed in the "Results and discussion" section.

Aerosol chemical characterization

The aerosol's chemistry affects its potential corrosiveness (Lau et al. 2008; Wan et al. 2002; Lobnig et al. 1994) and determines the values of DRH and CRH (Martin 2000; Martin et al. 2003; Seinfeld and Pandis 1998; Potukuchi and Wexler 1995). Thus, the second half of the $PM_{2.5}$ samples used in the AEC was chemically analysed to determine the aerosol chemical composition.

In this respect, the water-soluble inorganic aerosol fraction of the $PM_{2.5}$ samples was quantified using ion chromatography (IC). Cations (Na^+, NH_4^+, K^+, Mg^{2+}, Ca^{2+}) and anions (F^-, Cl^-, NO_3^-, SO_4^{2-}) were analysed using two coupled chromatography systems (Dionex ICS-90 and ICS-2000) served by a shared auto-sampler (AS3000, Dionex), after the extraction of $PM_{2.5}$ in 3 mL of ultrapure water (Milli-Q®; 18.2 MΩ cm @ 25 °C) for 20 min using an ultrasonic bath (SONICA®, Soltec, Italy). The obtained solutions were then filtered (0.45 µm PTFE Syringe Filters, Phenomenex) and analysed within the following 24 h. Extraction efficiencies have already been investigated in a previous work (Perrone et al. 2010); they are reported in the supplementary material (Table S1), together with a detailed description of the complete methodology adopted for the purposes of aerosol chemical characterization.

DRH and CRH modelling

In this section, we illustrate the methodology used to model DRH and CRH from our knowledge of the aerosol chemical composition. The main goal here is the real-time control of both DRH and CRH inside DCs, starting from the use of on-site fast aerosol chemical speciation techniques.

The aerosol's DRH values were estimated using the two most important thermodynamic models, namely: (1) the Extended Aerosol Inorganic Model (E-AIM Model-II) by Clegg et al. (1998) (http://www.aim.env.uea.ac.uk/aim/aim.php); (2) the ISORROPIA (II) code (Fountoukis and Nenes 2007) (http://isorropia.eas.gatech.edu/index.php?title=Main_Page).

E-AIM is a state-of-the-art aerosol thermodynamic model for the $H^+–NH_4^+–SO_4^{2-}–NO_3^-–H_2O$ composition of the aerosol. This model has been successfully used in the past to accurately predict aerosol acidity and DRH (Pathak et al. 2004).

ISORROPIA (II) calculates the composition and phase state of an $NH_4^+–SO_4^{2-}–NO_3^-–Cl–Na^+–Ca^{2+}–K^+–Mg^{2+}–H_2O$ inorganic aerosol (Fountoukis and Nenes 2007).

The main difference between the two is that the first provides the most accurate description of the thermodynamics of the system, while the second has been optimized and speeded up for computational applications (Zaveri et al. 2005; Seinfeld and Pandis 1998).

The aerosol's CRH values were modelled using a parametric approach (Martin et al. 2003) derived for a pure saline aerosol system of $SO_4^{2-}–NO_3^-–NH_4^+–H^+–H_2O$; therefore, it only considers homogeneous nucleation during crystal nuclei formation, while avoiding any consideration of the effects of different kinds of inclusions embedded within an aerosol particle (i.e. silicates, organics…) (Martin 2000).

The CRH model is composed of two different empirical equations. The first equation calculates the RH at which crystallization begins ($\mathrm{CRH}_{\mathrm{start}}$),

$$\begin{aligned} CRH_{start}(X,Y) = & -697.908 - 15.351X + 0.43X^2 \\ & - 22.11Y + 33.882XY - 1.818X^2Y \\ & + 0.772Y^2 - 1.636XY^2 \\ & + \frac{17707.6}{25 + (X - 0.7)(Y - 0.5)} \end{aligned} \quad (1)$$

where X is the ammonium fraction of the whole ammonium plus hydrogen $\left[\mathrm{NH}_4^+/\left(\mathrm{NH}_4^+ + \mathrm{H}_{\mathrm{tot}}^+\right)\right]$, and Y is the sulphate fraction of the whole sulphate plus nitrate $[\mathrm{SO_4}^{2-}/(\mathrm{SO_4}^{2-}+\mathrm{NO_3}^-)]$.

The second equation in the Martin et al. (2003) model concerns the RH at which the crystallization process ends ($\mathrm{CRH}_{\mathrm{end}}$),

$$\begin{aligned} CRH_{end}(X,Y) = & \; 3143.44 + 63.07X + 0.114X^2 + 87.97Y \\ & - 125.73XY + 0.586X^2Y + 0.95Y^2 \\ & - 1.384XY^2 - \frac{79692.5}{25 + (X - 0.7)(Y - 0.5)} \end{aligned} \quad (2)$$

Finally, both $\mathrm{CRH}_{\mathrm{start}}$ and $\mathrm{CRH}_{\mathrm{end}}$ refer to a temperature of 20 °C. Since the AEC measurements were conducted at 25 °C, and given the CRH values that were estimated by the model (see the "Results and discussion" section), we consider this difference to be negligible for the purposes of the present work.

DC's case study

As reported in section "Introduction", the ASHRAE's white papers (2009 and 2011) set out thermodynamic guidelines for DCs concerning the air supply: the "allowable" range is 15–32 °C (20–80 % of RH with a maximum dew point of 17 °C), while the "recommended" range is 18–27 °C (5.5 °C of dew point–60 % of RH and a maximum dew point of 15 °C). However, they are of a general nature and do not take account of the aerosol's DRH and CRH in a given location. Hence, there is the need for the development of new thermodynamic areas of operation at each DC construction site.

In this study, the DRH and CRH values obtained through conductivity measurements were applied to the design of a DC created for the Italian National Hydrocarbon Institution (Eni). The main aim was to prevent aerosol hydration already at the entrance to the DC, while at the same time obtaining an energy benefit by developing a proper thermodynamic operating area for the DFC.

The investigated DC was the *Eni Green Data Center* (GDC-Eni; http://www.eni.com/green-data-center/it_IT/pages/home.shtml) located in Italy's Po Valley; this DC was designed to operate with a DFC cycle for energy-saving purposes. The GDC-Eni became operative in December 2013, and is designed to centralize all of Eni's management IT. A total area of 5,200 m^2 of IT is present, with a final installed power of 30 MW (5.8 kW m^{-2}). To ensure the effective cooling of the system, an airflow rate of about 8×10^6 m^3 h^{-1} is provided, with a T set-point of 25 °C, as it has been demonstrated that above this temperature the demand for internal fan power for cooling purposes increases exponentially (ASHRAE 2011). The warming of the air supply by Information Technology (IT) at the GDC-Eni depends on the type of computers used, their utilization and status, and ranges from between 2 and 20 °C. The individual components (i.e. CPU, RAM, discs, connections…) operate at a temperature of between 35 and 90 °C (the latter temperature in the case of the CPU). These values are in line with those reported in the literature; Dogrouz and Nagulapally (2009) reported a temperature range of about 40–100 °C on the surface of printed circuit boards, depending on the component in question. A similar work (Shankaran et al. 2010) reported a lower temperature range of between 25 and 50 °C. Therefore, the aforementioned data highlight the presence of surface heating characterized by high spatial heterogeneity, which results in a reduction in RH at the circuit board level.

However, as reported in the "DRH and CRH measurements" section, both DRH and CRH vary with temperature (Onasch et al. 1999; Seinfeld and Pandis 1998); thus, as with RH, they will vary within the DC with a high degree of spatial heterogeneity. For this reason, the present work refers to the thermodynamic characteristics of the supply air only, as this approach allows the whole DC to be protected (see the demonstration in the "Results and discussion" section).

The energy performance of the GDC-Eni has been evaluated in the present study using Power Usage Effectiveness (PUE) calculated as follows (Shehabi 2009),

$$\mathrm{PUE} = \frac{\text{Total Electricity Load of Building}}{\text{IT Electricity Load}} \quad (3)$$

The PUE ratio equals 1.0 when the entire electricity supply is taken up by IT equipment, while a PUE of 2.0 indicates that the building's electricity intake is the same as the IT's electricity requirements.

Details of the PUE calculation are reported in the supplementary material, while a complete description of the characteristics of the GDC-Eni, together with an initial feasibility study, is reported in Ferrero et al. (2013).

Results and discussion

DRH and CRH were measured in the AEC and modelled from aerosol chemical composition on an ensemble of 55

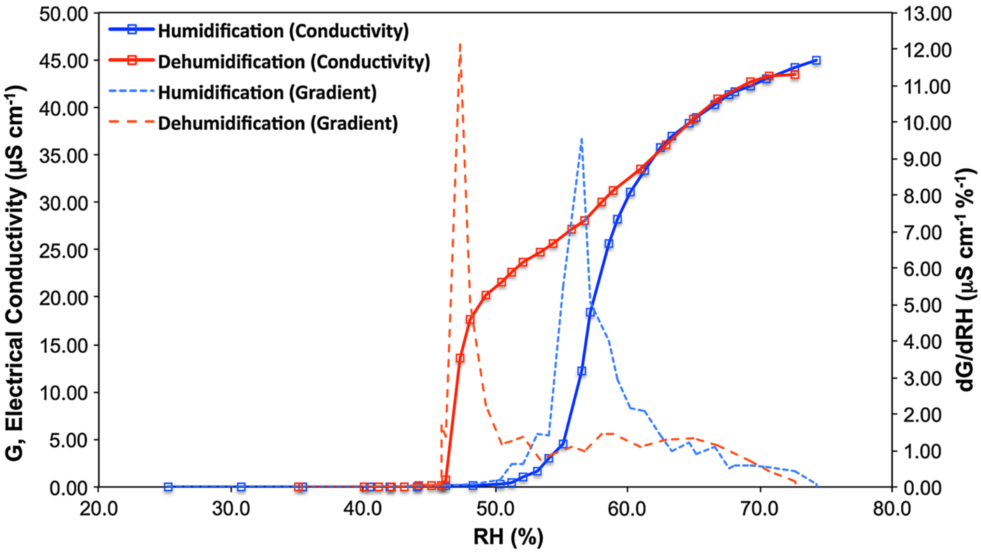

Fig. 1 Conductivity graphs and the corresponding gradient curves for the $PM_{2.5}$ sample collected at Torre Sarca on March 14, 2009; a clearly visible hysteresis cycle is present

$PM_{2.5}$ samples, collected at TS over the course of the four seasons between 2006 and 2009, and stored in the Filter Bank at the University of Milano-Bicocca. The following sections of this work are going to examine the conductivity measurements, and the method of determining DRHs and CRHs and their ambient values. A comparison between experimental and modelled values is also offered, together with a discussion of the implications of the aforementioned results for DCs. All averaged data are reported here as mean ± mean standard deviations.

Measured ambient DRH and CRH

Conductivity measurements in the AEC: minimum aerosol loading

Conductivity measurements were carried out in the AEC on ambient $PM_{2.5}$ samples collected at the TS site. The majority of $PM_{2.5}$ samples investigated in the AEC displayed electrical conductivity responses to RH changes during both humidification and dehumidification (Fig. 1). In fact, only 10 $PM_{2.5}$ samples out of the entire 55-filter ensemble (18 % of all investigated samples) revealed no signal in the AEC while RH was varied.

Thus, we firstly examine the minimum aerosol loading required in order to perform conductivity measurements with the experimental configuration (AEC + $PM_{2.5}$ sampling) described in the "Materials and methods" section.

As a matter of fact, such behaviour was not previously reported either in Yang et al. (2006) or in Song et al. (2013). However, the experimental measurements of both the aforesaid studies were conducted in saturating conditions of aerosols on the investigated media, namely: Whatman filter paper soaked with saturated ionic solution (Yang et al. 2006), and an electric coupon test with 150–600 µg cm^{-2} of aerosol deposited (Song et al. 2013), respectively.

Conversely, in the present study, the total aerosol mass loading on the sampled filters varied with $PM_{2.5}$ ambient concentrations. The 55 $PM_{2.5}$ samples considered in this work span a range of atmospheric concentrations of between 13.7 and 107.5 µg m^{-3}. These are typical values for the Po Valley, which is characterized by seasonally modulated pollution (Ferrero et al. 2011b; Carbone et al. 2010). Moreover, they turn into a similarly broad range of aerosol loading on the sampled $PM_{2.5}$ filters (24 h sampling time; flow 2.3 m^3 h^{-1}), from 63.2 µg cm^{-2} (0.755 mg on filters) to 496.6 µg cm^{-2} (5.932 mg on filters). Our range comprises values both below and above the minimum surficial aerosol deposition used by Song et al. (2013).

Following this observation, the aerosol mass load on such filter samples, together with the total ionic fraction content, was investigated in order to determine minimum aerosol loading, so as to ensure detection of conductivity changes while varying the RH in the AEC.

The average aerosol loading on the 45 $PM_{2.5}$ samples subset revealing electrical conductivity responses was 221.9 ± 13.5 µg cm^{-2} (2.651 ± 0.161 mg on filters), a figure slightly higher than the lower surficial dose used by Song et al. (2013); conversely, the 10 $PM_{2.5}$ samples subset that did not show any electrical conductivity response, displayed a statistically lower (*t* Student at $\propto = 0.01$) aerosol mass loading, with a value of 127.1 ± 7.8 µg cm^{-2} (1.518 ± 0.094 mg on filters). Due to the important role of the aerosol ionic fraction in determining electrical signal conduction, the average ion loading on both PM$_{2.5}$ sample subsets was also addressed: 85.7 ± 9.2 μg cm^{-2} (1.023 ± 0.110 mg on filters) for those samples that showed electrical conductivity responses to RH changes, and 53.1 ± 6.5 μg cm^{-2} (0.634 ± 0.077 mg on filters), for those that did not.

A value similar to the latter one can be derived by linearly correlating the ionic surficial loading of the PM$_{2.5}$ sample subset displaying an electrical conductivity response (y), with conductivity measurements (x) at 80 % of RH; the intercept of the linear regression thus obtained ($y = 1.8x + 50.0$; not shown) permits estimation of the minimum ionic surficial mass below which no electric signals were detected: 50.0 μg cm^{-2}. It is worth noting that the ionic surficial loading for the 10 filters that did not show any signal, is not far off the theoretical value (24.2 μg cm^{-2}) estimated by Weschler (1991) for pure 520 nm NH_4HSO_4 particles on the basis of the percolation theory (Hoschen and Kopelman 1976; Hoschen et al. 1978). However, as Tencer (2008) reported, the value at which the aerosol starts to conduct the electrical signal and at which a bridging process commences, may vary according to the geographical region and the related aerosol properties (chemistry and size).

Thus, by following the aforementioned approach, but considering the whole PM$_{2.5}$ mass rather than the ionic fraction mass only, as the "y" variable, the minimum PM$_{2.5}$ mass for detection of an electrical signal proved to be an average daily PM$_{2.5}$ concentration of 27.5 μg m^{-3} in Milan. Data from ARPA-Lombardia (the Lombardy regional branch of the Italian Regional Environmental Protection Agency) show that this concentration is exceeded in Milan on more than 70 % of winter days, and on 34 % of all days throughout the year. However, the minimum aerosol loading limit could be overcome simply by changing the sampling procedure. For example, by collecting aerosol for periods of more than 24 h, or by concentrating the 24-hour sample on a smaller filter surface. Moreover, a high-volume-sampler (flow > 6 m^3 h^{-1}) should be used rather than an LVS.

Conductivity measurements in the AEC: DRH and CRH determination

Figure 1 shows a case study of conductivity measurements carried out in the AEC for a PM$_{2.5}$ sample (57 μg m^{-3}) collected on March 14, 2009; conductivity curves are reported as a function of the RH during both humidification and dehumidification.

Conductivity graphs (Fig. 1) show a typical example of a hysteresis cycle of the aerosol and allow different regions to be distinguished on the basis of the aerosol's interaction with water. Along the humidification curve (Fig. 2, blue line), a dry region is followed first by a deliquescent region (sharp increase of conductivity; $\Delta G \sim 20$ μs cm^{-1}), and then by a hygroscopic growth region (due to continuous condensation of water); the reverse happens during dehumidification (Fig. 2, red line), when evaporation took place, followed by crystallization (sharp decrease in conductivity; G fell almost to 0), which in turn led once again to a dry state.

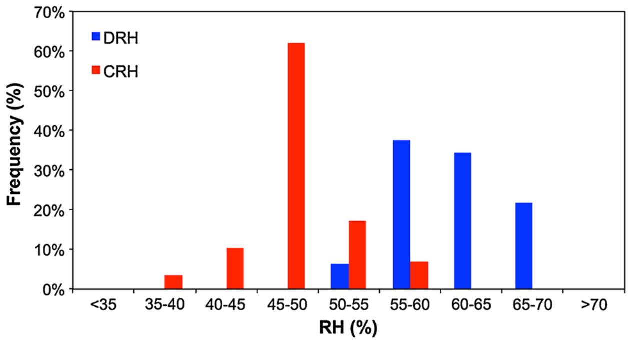

Fig. 2 Frequency histograms for ambient DRH and CRH measured over the whole PM$_{2.5}$ sample set

The deliquescence and crystallization regions shown in Fig. 1 represent the RH ranges corresponding to a phase change for the aerosol water-soluble compounds: from solid to liquid (for DRH) and vice versa (for CRH), as many scholars have pointed out (Martin 2000; Seinfeld and Pandis 1998; Potukuchi and Wexler 1995).

The conductivity graphs reported in Fig. 1 are in keeping with the shape of those conductivity measurements reported by Yang et al. (2006) and by Song et al. (2013). However, while Yang et al. (2006) determined the DRHs as the mid-point of the RHs, where the largest change in conductivity was observed (due to the lower RH resolution steps), Song et al. (2013) did not estimate any DRH values, but defined a critical transition range (a proxy of the DRH region) as the RH range to be found between the start of impedance degradation (increase in conductivity) and the Failure Threshold Level (FTL) of 1 MΩ.

This lack of any common methodology enables us to introduce an operational definition to be adopted when determining DRH and CRH using a conductivity method: DRH and CRH correspond to the RHs at which the absolute value of the conductivity gradient reaches its maximum level (marked by a sharp change in the electric signal); moreover, the corresponding deliquescence and crystallization regions are to be found within the ranges of RH in which the gradient values deviate significantly from zero and contain its maximum. As reported by Yang et al. (2006), the conductivity method is not overly sensitive to deviations of the mixture composition from the eutonic value (Yang et al. 2006); thus, the DRH and CRH values determined as above encapsulate the overall complexity of the ambient aerosol's chemistry. Finally, as a result of the fact that DRH should not be confused with hygroscopic growth, which is the condensation of water vapour on an aerosol in the liquid phase while relative humidity increases (Martin 2000), the proposed definition includes a strict determination of the DRH region, thus enabling us to separate it from the following hygroscopic growth region (Fig. 1). The same also happens in the case of CRH, which results separate from the previous evaporation region (Fig. 1).

The gradient method was applied to the conductivity graphs obtained from the $PM_{2.5}$ sample response measured inside the AEC. For the case study showed in Fig. 1, DRH and CRH occurred, respectively, at 57.0 % (region: 50.3–62.5 %) and at 47.0 % (region: 49.0–46.0 %) of RH.

Thus, first of all the proposed approach enables us to accurately determine DRH and CRH by combining standardized and certified methods of aerosol sampling ($PM_{2.5}$ EN-14907) with conductivity measurements taken in the AEC. Moreover, this method allows us to work "off-line" from the sampling activity, making it possible to determine previous values of DRH and CRH from samples stored in filter bank archives. Results in terms of ambient DRHs and CRHs for the whole ensemble of $PM_{2.5}$ samples are reported in the following section.

Ambient DRHs and CRHs

Electrical conductivity measurements evidenced the presence of a hysteresis cycle (as reported in Fig. 1). The frequency distributions for both DRH and CRH were calculated for the whole $PM_{2.5}$ ensemble and are shown in Fig. 2.

DRHs vary from 50 to 70 %, while CRHs vary from 35 to 60 %. The most abundant DRH_s were found in the 55–60 and 60–65 % ranges (with a frequency of 38 and 34 %, respectively), while the most abundant CRH_s lay in the 45–50 % range (with a frequency of 62 %).

Thus, the mean values of DRH and CRH were 60.5 ± 0.8 % (transition region: 56.9 ± 1.0–64.5 ± 1.0 %) and 47.9 ± 0.7 % (transition region: 49.9 ± 0.6–45.3 ± 0.7 %), respectively, accounting for an average hysteresis amplitude (the difference between DRH and CRH) of 11.7 ± 0.8 %.

The latter result is very important as it indicates the dependence of particle hydration on RH history: in the Po Valley, the atmospheric aerosol can be hydrated even if the RH of the surrounding air is below the DRH.

Thus, in order to predict the aerosol phase (dry or hydrated) on the basis of the time trend of RH, meteorological data for the Milan area were used together with the mean DRH (60.5 ± 0.8 %) and CRH values (47.9 ± 0.7 %), to calculate the percentage frequencies of the aerosol phase for the period 2006–2009. For the purposes of this calculation, all Milan RH data were reported at a temperature of 25 °C, as this represents the GDC-Eni's set-point temperature.

Results showed that: (1) 52 % of the time the aerosol was dry, due to a RH lower than the CRH (36 %) or an increasing RH lying between the CRH and DRH (16 %); and (2) 48 % of the time the aerosol was hydrated, due to a RH higher than the DRH (39 %) or a decreasing RH lying between the DRH and the CRH (9 %).

Thus, if only DRH is considered when optimizing a DC's cooling cycle, as required by the ASHRAE guidelines, there is a risk of failing to consider the fact that the aerosol is hydrated for the period during which RH is decreasing between DRH and CRH; for the purposes of the present GDC-Eni case study, this risk is present approximately 9 % of the time.

This knowledge is of fundamental importance for the prevention of aerosol corrosion in DCs. Moreover, in order to guarantee corrosion prevention effectiveness, DRH and CRH should be dynamically controlled on the basis of the aerosol's chemical composition. The latter point is discussed in the following section.

Modelled DRHs and CRHs: comparison with AEC data

Results reported in the previous section highlight the need for the real-time dynamic control of the best DFC operating condition in a free-cooled DC, in order to prevent aerosol hydration even before its deposition on electronic circuitry. In order to combine this need with energy-saving requirements, such an approach would have to be based on the continuous monitoring of both DRH and CRH with the highest possible time resolution. However, up to now, the conductivity approach reported in this paper consists in an off-line technique. One way of overcoming this limitation is to estimate both DRH and CRH along time by means of modelling activity, starting from our knowledge of the aerosol's chemistry. In fact, aerosol ionic fraction determination at a high time resolution (i.e. through the use of aerosol mass spectrometers) is not currently a limiting factor (Jayne et al. 2000).

Thus, the aim of the following comparisons with model results is to understand their ability to predict both DRH and CRH simply starting from a fraction (39.4 ± 2.2 %, ionic fraction) of the whole aerosol's chemical composition.

DRH comparison

AEC experimental DRH data were compared with the results from two different models: ISORROPIA II and

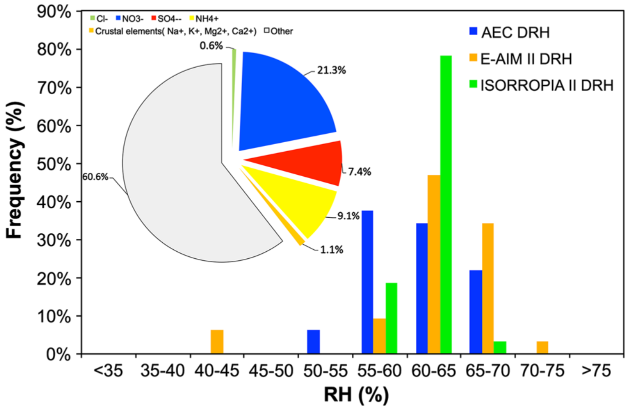

Fig. 3 This figure compares frequency histograms for DRH values measured in the AEC and calculated using the E-AIM II and ISORROPIA II models and shows the mean chemical composition for the $PM_{2.5}$ samples

E-AIM II. $PM_{2.5}$ chemistry (Table S1, supplementary material) were used as the input parameter to drive both models; simulations were conducted at 25 °C, the same temperature as that of the AEC data.

Figure 3 shows both the DRH frequency distributions for ISORROPIA II, E-AIM II and AEC data, together with the mean $PM_{2.5}$ chemical composition. It should be pointed out that E-AIM II predicts a wider range of DRH values, extending from 45 to 75 % of RH, while ISORROPIA II outputs lie along a narrower distribution (DRHs, 55–70 %). Their accuracy in predicting mean DRH values is shown in Table S2 (supplementary material), which shows averaged values for the start and end points of the deliquescence region, and for the values of DRH estimated by each model. Mean DRH values calculated using E-AIM II (61.5 ± 1.1 %) and ISORROPIA II (60.3 ± 0.2 %) only slightly exceed the mean experimental DRH (60.5 ± 0.8 %).

These three values, all close to 60 %, can be related to the aerosol chemistry. Table S1 (supplementary material) reports values of the aerosol ionic fraction, which was dominated by nitrates (21.3 ± 1.8 % of $PM_{2.5}$ mass), sulphates (7.4 ± 0.6 % of $PM_{2.5}$ mass) and ammonium (9.1 ± 0.5 % of $PM_{2.5}$ mass); nitrates were approximately 5 times greater than sulphates in terms of nmol m^{-3}. Moreover, Table S1 also shows a substantial balance between acids and bases, to be expected for a neutral (non-acidic) aerosol. Thus, in keeping with the literature (Seinfeld and Pandis 1998; Potukuchi and Wexler 1995), the DRH values (both experimental and modelled) can be explained by the higher nitrate content of a neutral aerosol.

Even if the mean experimental and modelled values were very similar and in line with the aerosol chemistry, the accuracy of the prediction for each single value, and not only for the averaged value, is crucial when considering a possible application for determining DRH at a high time resolution. From this perspective, performance evaluation parameters (Bias, Absolute Bias, RMSE) are also shown in Table S2 for both modelling results. Even if the two models' mean DRH values substantially correspond to the mean experimental values, the analysis of RMSE (6.3 %, for E-AIM II and 3.6 % for ISORROPIA II) together with bias (0.9 %, for E-AIM II and −0.2 % for ISORROPIA II) and absolute bias values (4.3 %, for E-AIM II and 2.8 % for ISORROPIA II) showed that there is a degree of compensation between positive and negative models' prediction errors. In fact, absolute bias is almost always higher than bias.

These results showed that, despite certain discrepancies, both models should be adopted by DCs in order to dynamically control DFC cycles.

As a final control, the hygroscopic growth behaviour (above the DRH region), dominated by the continuous condensation of water in the aerosol phase, was also investigated. Thus, data from E-AIM II and ISORROPIA II at 80 % of RH (above DRHs) were used to estimate the total mass of water condensed onto each $PM_{2.5}$ sample and to calculate the mass hygroscopic growth factor (HGf) as follows:

$$\mathrm{HGf} = \frac{\mathrm{PM}_{2.5} + \mathrm{mH_2O}_{(80\%)}}{\mathrm{PM}_{2.5}} \tag{4}$$

where $PM_{2.5}$ refers to the dry mass of the sampled aerosol, while $mH_2O_{(80\ \%)}$ indicates the water mass that is expected to condense on the aerosol at a RH of 80 %.

This estimation permitted a comparison with the modelling outputs also within the hygroscopic growth region, by comparing calculated HGf (Eq. 4) with the figures reported in the literature.

The mean estimated mass HGf was 1.49 ± 0.03 for E-AIM II and 1.48 ± 0.03 for ISORROPIA II. These figures are in keeping with the growth factors reported for the Po Valley by Svenningsson et al. (1992) and by Bialek et al. (2013), who measured HGfs of 1.44 ± 0.14 and 1.46, respectively.

CRH comparison

The AEC's experimental CRH data were also compared with the outputs obtained from the parametric model described in Martin et al. (2003). Once again, $PM_{2.5}$ chemistry (Fig. 3, Table S1) was used as an input parameter driving the model.

With reference to Eqs. 1 and 2, all samples with measured experimental CRH have $X = 1$ and variable Y values. Martin et al. (2003) states that the $[X,Y]$ domain of applicability is such that $\mathrm{CRH}(X,Y) \geq 1$ %. Assuming that X is constant and equal to 1, this limit results in a minimum value of 0.25 for the *Y* parameter. Of the whole $PM_{2.5}$ ensemble investigated in the AEC, only 12 $PM_{2.5}$ samples exceeded this critical value because, as shown in Fig. 3 (Table S1), the $PM_{2.5}$ samples were richer in nitrates than they were in sulphates. The mean *Y* value for these 12 samples was 0.32 ± 0.04, while for the entire dataset, the mean value of *Y* was 0.24 ± 0.03. Moreover, a comparison between these two data sets was only made for the starting (CRH_{start}) and end (CRH_{end}) points of the crystallization region, in accordance with the output of the model that did not permit the calculation of any crystallization curve. Table S3 (supplementary material) reports such a comparison for the aforementioned 12 samples. The average modelled CRH_{start} (18.7 %) differs by 32.7 % of RH from the experimental one (51.4 %), and there is a 28.2 % gap (17.3 and 45.5 %, modelled and measured, respectively) between the two CRH_{end}. Martin (2000) points out that the presence of metal oxides (i.e. Fe_2O_3, TiO_2…) in the aerosol's particles can lead to a CRH increase of up to 32 % more compared to a pure saline aerosol (i.e. pure $(NH_4)_2SO_4$), because such oxides can act as crystallization nuclei driving heterogeneous nucleation, which results in crystallization at higher RH values. Furthermore, the presence of organic material, such as glycerol or certain carboxylic acids, can also increase the aerosol's CRH (Choi and Chan 2002). Previous element and carboxylic acid quantification for $PM_{2.5}$ at the Milan TS site during the same period was performed by Perrone et al. (2013): they found concentrations of 549 ± 189 ng m^{-3}(1.6 ± 0.3 % of $PM_{2.5}$) and of 389 ± 133 ng m^{-3} (1.1 ± 0.4 % of $PM_{2.5}$), respectively. In the light of such data, it is likely that insoluble inclusions and organic matter cause the difference witnessed between experimental and model CRH values.

Thus, for CRH, considering the differences between measured and modelled results, the parametric model—which was developed for inorganic ion data only—is not suitable for the simulation of the CRH of the complex ambient aerosol, and it cannot be adopted in DCs in order to dynamically control DFC cycles. Thus, further investigation is required with regard to this in order to account for the effect of inclusions on the modelled CRH.

Implications for data centers

The results reported in the previous sections show that a continuous condensation of water in the aerosol phase starts from the DRH doing increase the aerosol conductivity. Hence, the modelling simulations were used to determine the relationship between the modelled condensed water, as calculated by both E-AIM II and ISORROPIA II, and the measured conductivity above the DRH. The resulting correlations are shown in Fig. 4, which indicates an increase in conductivity of approximately $0.615 - 0.798\ \mu S\ cm^{-1} \mu mol^{-1}_{H2O}$, depending on the model output. Thus, as an increase in the conductivity of atmospheric particles may lead to bridging, the aforementioned results highlight the need to maintain the aerosol entering into a DC in the dry state prior to any deposition on IT.

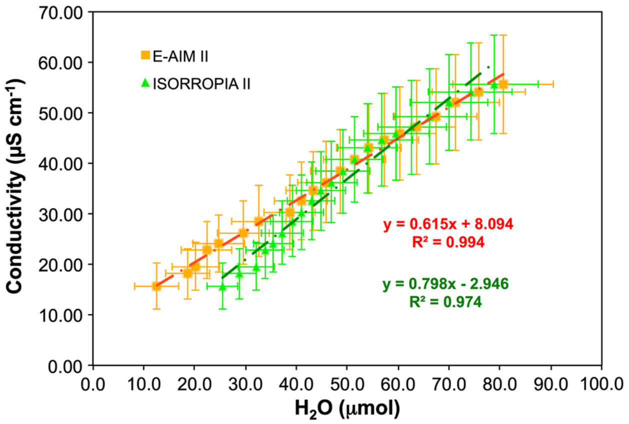

Fig. 4 Linear correlation between the averaged conductivity measured in the AEC and the average quantity of condensed water as estimated by ISORROPIA II and E-AIM II

Therefore, the experimental results (DRH and CRH) obtained from AEC measurements were used here to define the best DFC cycle applicable to the GDC-Eni.

The DFC operating area optimized the "allowable" ASHRAE values. The lower moisture limits of ASHRAE (20 % of RH) were maintained to enhance energy efficiency, while the upper RH limit was set between 48 and 60 %, depending on the RH history according to the ambient values of both DRH and CRH. The use of a maximum dew point limit was avoided, as it does not affect the hydration level of the aerosol. Finally, the lower ASHRAE temperature limit (15 °C) was maintained in order to enhance energy efficiency, while the upper *T* limit was set at 25 °C according to the GDC-Eni design (see the "Materials and methods" section). Figure 5 shows the DFC operating area inside the GDC-Eni; even though the reported area is site specific, the methodology used to determine it is of general application.

The DFC operating area reported in Fig. 5 refers to the cooling air supply in the GDC-Eni. However, as reported in the "DCs case study" section, a *T* increase at the circuit board reflects on both aerosol properties and RH changes in a spatially heterogeneous manner. Therefore, it is necessary to understand whether a higher *T* close to the surface of a circuit board would lead to a lower or higher risk of aerosol hydration. In order to answer this question, the E-AIM II and ISORROPIA II models (previously validated) were used to predict, at increasing T, the DRH of an

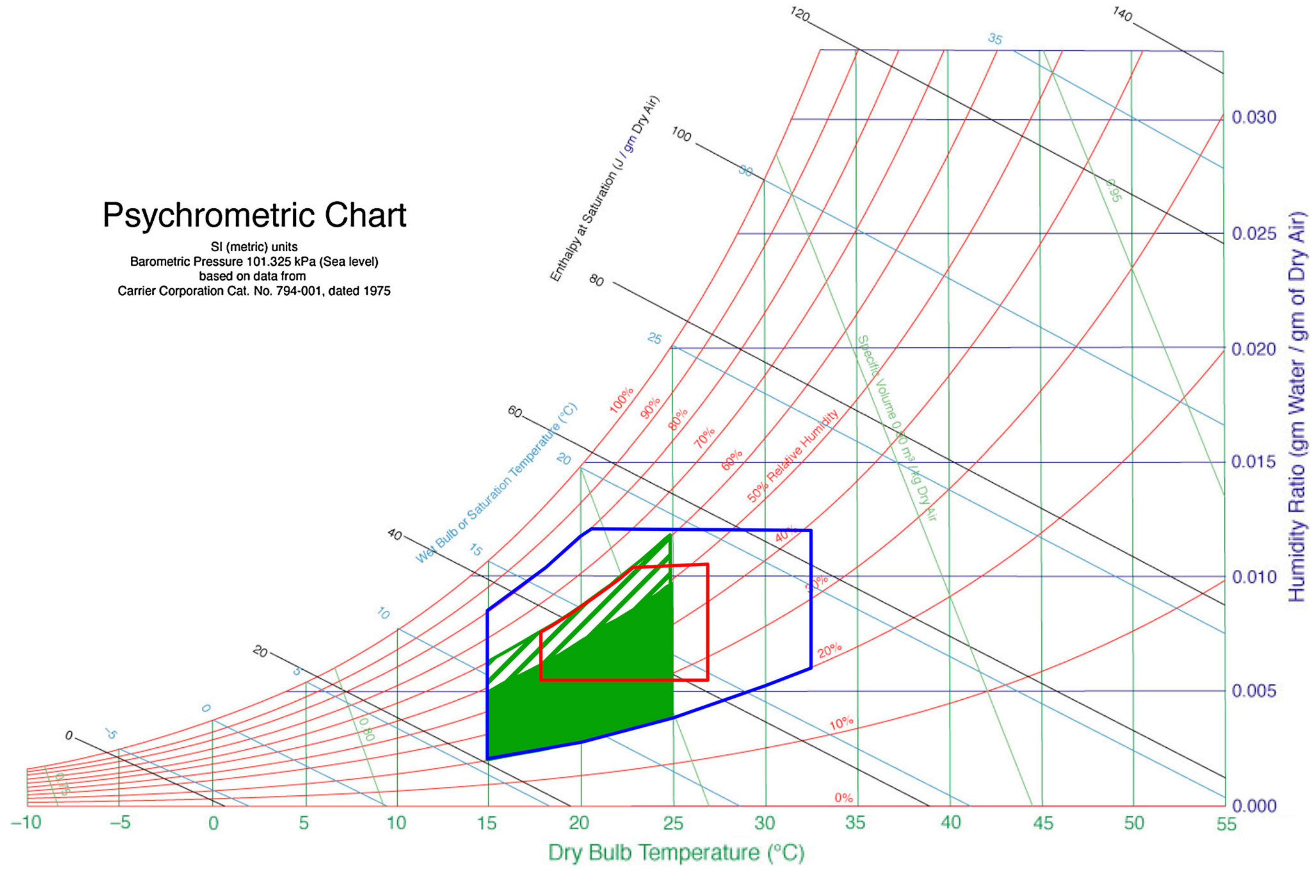

Fig. 5 Psychrometric chart of the GDC-Eni's thermodynamic operating area, the *full green line* indicates the area below the CRH, while the *dashed green lines* indicate the area between the CRH and the DRH where the application of DFC depends on the RH history. ASHRAE's "allowable" (*blue*) and "recommended" (*red*) areas are also plotted

aerosol with the same chemical composition reported in Fig. 3 and Table S1. Results were compared with the expected lowering of RH at the same T. The starting condition was the upper limit for the GDC-Eni: 60 % of RH at 25 °C (worst case scenario). Results are reported in the supplementary material in Figure S2: a greater impact of *T* on RH, rather than on DRH, was observed. Thus, the use of common thermodynamic limits (RH and *T*) for the cooling air supply helps avoid deliquescence throughout the entire DC. The aforementioned results are the main reason why the approach reported in the present study refers to the thermodynamic characteristics of the supply air only.

Thus, the DFC's calculated operating area allows aerosol hydration to be avoided and energy to be saved at one and the same time; in fact, air-conditioning is not necessary when ambient conditions permit the safe application of DFC. Thus, in order to estimate the energy saving of the GDC-Eni, the DC's energy consumption was calculated using Eq. 3 (see also supplementary material) considering the time frequencies of different aerosol hydration states for the period 2006–2009.

As a result, the GDC-Eni PUE (Eq. 3) was calculated to be 1.22. This means that in 1 year the calculated energy saving (compared to traditional DCs with a PUE of 2.04) for the entire GDC-Eni (30 MW of IT) is estimated to be 215 GWh (79 %). This turns into both environment and economic savings: 78 kt of CO_2 not emitted and € 26 mln saved (considering a CO_2 emission factor of 362 $gCO_2\ kWh^{-1}$ http://www.eea.europa.eu/ and an energy cost of 0.15 € kWh^{-1}).

Conclusion

This study develops an innovative method of determining both aerosol deliquescence and crystallization relative humidities, by combining standardized aerosol sampling techniques ($PM_{2.5}$; EN-14907) with the assessment of the electrical effect of the aerosol depending on the relative humidity.

An AEC was specifically designed for this purpose, and conductivity measurements were taken on $PM_{2.5}$ samples while varying RH in the chamber.

Conductivity graphs showed a sharp change in conductivity in correspondence to the deliquescence and the crystallization processes; thus, a gradient method was introduced to determine both the deliquescence and crystallization relative humidities, and the corresponding regions of aerosol phase transition (from solid to liquid and vice versa).

The first deliquescence and crystallization relative humidities for the Po Valley were determined as: 60.5 ± 0.8 % (transition region: 56.9 ± 1.0–64.5 ± 1.0 %) and 47.9 ± 0.7 % (transition region: 49.9 ± 0.6–45.3 ± 0.7 %). These results highlight the presence of a hysteresis cycle of the aerosol, which is of considerable importance for DCs.

The aforementioned results made it possible to identify a critical area of operation for a direct free-cooling application at a DC designed for the Italian National Oil and Gas Company (Eni). Aerosol hydration, and thus aerosol corrosion, was avoided, while at the same time, a large amount of energy was saved due to the use of outdoor air (instead of air-conditioning) to cool the information technology. A potential energy saving of 79 % over a traditional air-conditioning cooling system was estimated; this represents a saving of 215 GWh of energy and a reduction of 78 kt in the emission of equivalent CO_2 per year. This energy saving is site specific, but the innovative methodology used in this study to obtain this result is of general application.

Moreover, in order to lay the foundations for a real-time estimation of the aerosol hydration state within a DC, measurements conducted in the AEC were compared to simulations performed using E-AIM II and ISORROPIA II models (for deliquescence) and a parametric model (for crystallization).

Results point to a good model-to-measurements agreement for deliquescence, while in the case of crystallization, the model simulations were a way of representing the whole aerosol's behaviour.

Finally, during this study, several objectives of the European Horizon 2020 Directive (CO_2 emission reduction, energy efficiency) were reached, thus offering a good example of the way in which the prevention of risks associated with the presence of atmospheric aerosol can also result in considerable energy savings and cost reductions, together with the substantial protection of the environment.

Acknowledgments The authors are grateful to the SINOPIAE project (Grant Number: E47I11000520004) funded by the Italian Lombardy Region within the framework of the European Fund for Regional Development FESR 2007–2013. The authors would like to thank the two anonymous reviewers who helped improve the quality of the paper. Finally, this work is dedicated to the memory of Luigi Casati and Maria Luisa Janes.

References

ASHRAE (2009) Gaseous and particulate contamination guidelines for data centers. Whitepaper prepared by ASHRAE Technical Committee (TC) 9.9 Mission Critical Facilities, Technology Spaces, and Electronic Equipment. http://www.Eni.com/green-data-center/it_IT/static/pdf/ASHRAE_2.pdf

ASHRAE (2011) Gaseous and particulate contamination guidelines for data centers. Whitepaper prepared by ASHRAE Technical Committee (TC) 9.9 Mission Critical Facilities, Technology Spaces, and Electronic Equipment. http://ebookbrowse.com/gdoc.php?id=191780893&url=3ba7e0c6a7c2ae744b9103d45d02e282

Bialek J, Dall'Osto M, Vaattovaara P, Decesari S, Laaksonen A, O'Dowd C (2013) Hygroscopic and chemical characterisation of Po Valley aerosol. Atmos Chem Phys Disc 13:3247–3278

Carbone C, Decesari S, Mircea M, Giulianelli L, Finessi E, Rinaldi M, Fuzzi S, Marinoni A, Duchi R, Perrino C, Sargolini T, Vardè M, Sprovieri F, Gobbi GP, Angelini F, Facchini MC (2010) Size-resolved aerosol chemical composition over the Italian Peninsula during typical summer and winter conditions. Atmos Environ 44:5269–5278

Choi MY, Chan CK (2002) The effects of organic species on the hygroscopic behaviors of inorganic aerosols. Environ Sci Technol 36:2422–2428

Clegg SL, Brimblecombe P, Wexler AS (1998) Thermodynamic model of the system H+–NH4+–Na+–SO42–NO3–Cl–H2O at 298.15 K. J Phys Chem A 102:2155–2171

Di Nicolantonio W, Cacciari A, Petritoli A, Carnevale C, Pisoni E, Volta ML, Stocchi P, Curci G, Bolzacchini E, Ferrero L, Ananasso C, Tomasi C (2009) MODIS and OMI satellite observations supporting air quality monitoring. Radiat Prot Dosim 137:280–287

Dogrouz MB, Nagulapally MK (2009) Effects of trace layers and Joule heating on the temperature distribution of printed circuit boards: a computational study. J Thermal Sci Eng Appl 1(2). doi:10.1115/1.4000286

Ferrero L, Bolzacchini E, Petraccone S, Perrone MG, Sangiorgi G, Lo Porto C, Lazzati Z, Ferrini B (2007) Vertical profiles of particulate matter over Milan during winter 2005/2006. Fresen Environ Bull 16:697–700

Ferrero L, Perrone MG, Petraccone S, Sangiorgi G, Ferrini BS, Lo Porto C, Lazzati Z, Cocchi D, Bruno F, Greco F, Riccio A, Bolzacchini E (2010) Vertically-resolved particle size distribution within and above the mixing layer over the Milan metropolitan area. Atmos Chem Phys 10:3915–3932

Ferrero L, Mocnik G, Ferrini BS, Perrone MG, Sangiorgi G, Bolzacchini E (2011a) Vertical profiles of aerosol absorption coefficient from micro-Aethalometer data and Mie calculation over Milan. Sci Total Environ 409:2824–2837

Ferrero L, Riccio A, Perrone MG, Sangiorgi G, Ferrini BS, Bolzacchini E (2011b) Mixing height determination by tethered balloon-based particle soundings and modeling simulations. Atmos Res 102:145–156

Ferrero L, Cappelletti D, Moroni B, Sangiorgi G, Perrone MG, Crocchianti S, Bolzacchini E (2012) Wintertime aerosol dynamics and chemical composition across the mixing layer over basin valleys. Atmos Environ 56:143–153

Ferrero L, Sangiorgi G, Ferrini BS, Perrone MG, Moscatelli M, D'Angelo L, Rovelli G, Ariatta A, Truccolo R, Bolzacchini E (2013) Aerosol corrosion prevention and energy-saving strategies in the design of green data centers. Environ Sci Technol 47(8):3856–3864

Ferrero L, Castelli M, Ferrini BS, Moscatelli M, Perrone MG, Sangiorgi G, Rovelli G, D'Angelo L, Moroni B, Scardazza

F, Mocnik G, Bolzacchini E, Petitta M, Cappelletti D (2014) Impact of black carbon aerosol over Italian basin valleys: high-resolution measurements along vertical profiles, radiative forcing and heating rate. Atmos Chem Phys 14:9641–9664

Fountoukis C, Nenes A (2007) ISORROPIA II: a computationally efficient thermodynamic equilibrium model for K^+–Ca^{2+}–Mg^{2+}–$NH_4{}^+$–Na^+–$SO_4{}^{2-}$–$NO_3{}^-$–Cl^-–H_2O aerosols. Atmos Chem Phys 7:4639–4659

Greenberg S, Mills E, Tschudi W, Rumsey P, Myatt B (2006) Best practices for data centers. Results from benchmarking 22 data centers. In: Proceedings of the 2006 ACEEE summer study on energy efficiency in buildings, Pacific Grove, CA, 13−18 Aug 2006. http://www.eceee.org/conference_proceedings/ACEEE_buildings/2006/Panel_3/p3_7/paper

Hong T, Koo C, Kim H (2012) A decision support model for improving a multi-family housing complex based on CO_2 emission from electricity consumption. J Environ Manag 112:67–78

Hoschen J, Kopelman R (1976) Percolation and cluster distribution. I. Cluster multiple labelling techniques and critical concentration algorithm. Phys Rev B 14:3438–3445

Hoschen J, Kopelman R, Monberg EM (1978) Percolation and cluster distribution. II. Layers, variable-range interactions and exciton cluster model. J Stat Phys 19:219–242

Jayne JT, Leard DC, Zhang X, Davidovits P, Smith KA, Kolb CE, Worsnop DR (2000) Development of an aerosol mass spectrometer for size and composition analysis of submicron particles. Aerosol Sci Technol 33(1–2):49–70

Koomey JG (2008) Worldwide electricity used in data centers. Environ Res Lett 3:1–8

Lau NT, Chan CK, Chan I, Fang M (2008) A microscopic study of the effects of particle size and composition of atmospheric aerosols on the corrosion of mild steel. Corros Sci 50:2927–2933

Leiva MA, Toro R, Morales RGE, Ríos MA, Gonzáles MR (2013) A study of water-soluble inorganic ions in size-segregated aerosols in atmospheric pollution episode. Int. J. Environ. Sci. Technol. doi:10.1007/s13762-013-0221-4

Litvak A, Gadgil AJ, Fisk WJ (2000) Hygroscopic fine mode particle deposition on electronic circuits and resulting degradation of circuit performance, an experimental study. Indoor Air 10:47–56

Lobnig RE, Frankenthal RP, Siconolfi DJ, Sinclair JD, Stratmann M (1994) Mechanism of atmospheric corrosion of copper in the presence of submicron ammonium sulfate particles at 300 and 373 K. J Electrochem Soc 141(11):2935–2941

Martin ST (2000) Phase transitions of aqueous atmospheric particles. Chem Rev 100:3403–3454

Martin ST, Schlenker JC, Malinowski A, Hung HM (2003) Crystallization of atmospheric sulfate-nitrate-ammonium particles. Geophys Res Lett 30(21). doi:10.1029/2003GL017930

Nazaroff WW (2004) Indoor particle dynamics. Indoor Air 14(7):175–183

Onasch TB, Siefert RL, Brooks SD, Prenni AJ, Murray B, Wilson MA, Tolbert MA (1999) Infrared spectroscopic study of the deliquescence and efflorescence of ammonium sulfate aerosol as a function of temperature. J Geophys Res 104:21317–21326

Otagiri M, Kutami M (2010) Trends of energy saving in data centers and Fujitsu group's approach. Fujitsu Sci Tech J 46(4):352–358

Owoade OK, Olise FS, Obioh IB, Olaniyi HB, Bolzacchini E, Ferrero L, Perrone G (2006) PM10 sampler deposited air particulates: ascertaining uniformity of sample on filter through rotated exposure to radiation. Nucl Instrum Meth A 564(1):315–318

Parolini L, Sinopoli B, Krogh BH, Wang Z (2012) A cyber-physical systems approach to data center modeling and control for energy efficiency. Proc IEEE 100(1):254–268

Pathak RK, Louie PKK, Chan CK (2004) Characteristics of aerosol acidity in Hong Kong. Atmos Environ 38:2965–2974

Perrone MG, Gualtieri M, Ferrero L, Lo Porto C, Udisti R, Bolzacchini E, Camatini M (2010) Seasonal variations in chemical composition and in vitro biological effects of fine PM from Milan. Chemosphere 78(11):1368–1377

Perrone MG, Larsen B, Ferrero L, Sangiorgi G, De Gennaro G, Udisti R, Zangrando R, Gambaro A, Bolzacchini E (2012) Sources of high PM2.5 concentrations in Milan, Northern Italy, molecular marker data and CMB modelling. Sci Total Environ 414:343–355

Perrone MG, Gualtieri M, Consonni V, Ferrero L, Sangiorgi G, Longhin E, Ballabio D, Bolzacchini E, Camatini M (2013) Particle size, chemical composition, seasons of the year and urban, rural or remote site origins as determinants of biological effects of particulate matter on pulmonary cells. Environ Pollut 176:215–227

Potukuchi S, Wexler A (1995) Identifying solid-aqueous-phase transitions in atmospheric aerosols. II. Acidic solutions. Atmos Environ 29(22):3357–3364

Randriamiarisoa H, Chazette P, Couvert P, Sanak J, Mégie G (2006) Relative humidity impact on aerosol parameters in a Paris suburban area. Atmos Chem Phys 6:1389–1407

Rodriguez S, Van Dingenen R, Putaud JP, Dell'Acqua A, Pey J, Querol X, Alastuey A, Chenery S, Ho KF, Harrison R, Tardivo R, Scarnato B, Gemelli V (2007) A study on the relationship between mass concentration, chemistry and number size distribution of urban fine aerosol in Milan, Barcelona and London. Atmos Chem Phys 7:2217–2232

Rood MJ, Covert DS, Larson TV (1987) Hygroscopic properties of atmospheric aerosol in Riverside, California. Tellus B 39(4):383–397

Sangiorgi G, Ferrero L, Perrone MG, Bolzacchini E, Duane M, Larsen BR (2011) Vertical distribution of hydrocarbons in the low troposphere below and above the mixing height: tethered balloon measurements in Milan, Italy. Environ Pollut 159(12):3545–3552

Seinfeld JH, Pandis SN (1998) Atmospheric chemistry and physics—from air pollution to climate change. Wiley, New Jersey

Shankaran GV, Dogruoz MB, deAraujo D (2010) Orthotropic thermal conductivity and joule heating effects on the temperature distribution of printed circuit boards. In: Proceeding of the 12th IEEE intersociety conference on thermal and thermomechanical phenomena in electronic systems, vol 1, pp 1–9

Shehabi A (2009) Energy demands and efficiency strategies in data center buildings. PhD Dissertation, Civil and Environmental Engineering, University of California, Berkeley

Shehabi A, Horvath A, Tschudi W, Gadgil AJ, Nazaroff WW (2008) Particle concentrations in data centers. Atmos Environ 42:5978–5990

Shehabi A, Ganguly S, Gundel LA, Horvath A, Kirchstetter TW, Lunden MM, Tschudi W, Gadgil AJ, Nazaroff WW (2010) Can combining economizers with improved filtration save energy and protect equipment in data centers? Build Environ 45:718–726

Shields HC, Weschler CJ (1998) Are indoor air pollutants threatening the reliability of your electronic equipment? Heat Pip Air Cond 70(5):46–54

Song B, Azarian MH, Pecht MG (2013) Effect of temperature and relative humidity on the impedance degradation of dust-contaminated electronics. J Electrochem Soc 160:C97–C105

Svenningsson IB, Hansson HC, Wiedensohler A, Ogren JA, Noone KJ, Hallberg A (1992) Hygroscopic growth of aerosol particles in the Po Valley. Tellus B 44:556–569

Syed S (2006) Atmospheric corrosion of materials. Emir J Eng Res 11:1–24

Tencer M (2008) Deposition of aerosol (''hygroscopic dust'') on electronics—mechanism and risk. Microelectron Reliab 48:584–593

Tschudi W, Xu T, Sartor D, Nordman B, Koomey J, Sezgen O (2004) Energy efficient data centers. Report LBNL-54163, 2004, Lawrence Berkeley National Laboratory, Berkeley, CA. http://www.osti.gov/bridge/servlets/purl/841561-aO7Lg9/native/841561.pdf

Wan Y, Yan C, Shi Z, Qu Q, Cao C (2002) Atmospheric corrosion of A3 steel with deposited ammonium sulfate. Acta Physico-Chimica 18(2):156–160

Weschler CJ (1991) Predictions of benefits and costs derived from improving indoor air quality in telephone switching offices. Indoor Air 1:65–78

Yang L, Pabalan RT, Juckett MR (2006) Deliquescence relative humidity measurements using an electrical conductivity method. J Solut Chem 35:583–604

Zaveri RA, Easter RC, Peters LK (2005) A computationally efficient multicomponent equilibrium solver for aerosols (MESA). J Geophys Res 110:D24203. doi:10.1029/2004JD005618